



Development of a Frost-Heave Testing Apparatus with a Triple Cell

Kean Thai Chhun¹ · Kyoung-Jea Jun² · Chan-Young Yune¹

Received: 22 November 2020 / Revised: 2 March 2021 / Accepted: 16 April 2021 / Published online: 29 April 2021
© Iran University of Science and Technology 2021

Abstract

In this study, the first frost-heave testing apparatus with a triple cell was developed that can measure the amount of frost-heave and heaving pressure, as well as achieve high-accuracy temperature control. The performance of the apparatus was validated by a series of frost-heave tests, which were conducted in a closed system with saturated sandy soil and an initial boundary temperature of 3 °C. The effect of having multiple cells (triple cell, double cell, and single cell), different freezing directions (top to bottom, both sides, and bottom to top), and multiple temperature gradients (0.09, 0.11, and 0.13 °C/mm), was examined to investigate the frost-heave properties of sandy soil. The reliability of the testing machine was validated by comparing the measured (experimental) and estimated (theoretical) amount of frost-heave that occurs in saturated sandy soil. The results show that the newly developed testing device accurately estimates the amount of frost-heave with error of < 8.69% between predicted and measured results for heaving pressure with freezing direction from top to bottom.

Keywords Frost-heave amount · Heaving pressure · Frost length · Frost-heave ratio · Freezing direction · Freezing temperature

Abbreviations

G_s	Specific gravity
H_f	Frost length
n	Porosity of the soil sample
T_l	Lower soil temperature
T_m	Setting temperature of the device
T_u	Upper soil temperature
$\gamma_{d,max}$	Maximum dry unit weight
$\gamma_{d,min}$	Minimum dry unit weight
η	Frost-heave ratio
Δh	Frost-heave amount

1 Introduction

In general, frost-heave is a natural phenomenon in which the formation of ice in soil causes expansion in both vertical and horizontal directions [1]. When saturated sand or gravel freezes, when there is no additional water supply and in undrained conditions, the pore water will increase in volume by about 9% after freezing [2]. Grain size distribution, temperature, overburden pressure, density, moisture content, and water supply are the factors that influence the frost-heave characteristics [3, 4]. In cold regions, frost-heave comes with a high risk of damage to infrastructure such as tunnels [5–7], highways [8, 9], railways [10, 11], pipelines [12, 13], and foundations [14]. Because of frost-heave, millions of US dollar are spent annually on the maintenance and rehabilitation of infrastructure [15]. Therefore, it is important to understand the mechanism of frost-heave if we are to reduce damage resulting from seasonal transition and maintenance cost.

To evaluate frost-heave properties, three types of testing devices were fabricated and standardized by those in the US [16], Japan [17], and the UK [18]. These are summarized in Table 1. The American Society for Testing and Materials [16] presented a testing apparatus to classify the susceptibility of frost-heave below the pavement (as shown in Fig. 1a), for frost-susceptible soils. The results for this

✉ Chan-Young Yune
yune@gwnu.ac.kr

Kean Thai Chhun
kt_chhun@yahoo.com

Kyoung-Jea Jun
lgnampyon@nate.com

¹ Department of Civil Engineering, Gangneung-Wonju National University, Jukheon-gil 7, Gangneung-si, Gangwon-do 25457, Republic of Korea

² Institute of Technology, Shinhwa Construction Co., Nambu-ro 62, Gangneung-si, Gangwon-do 25604, Republic of Korea

Table 1 Characteristics of three kinds of frost-heave test apparatus

Categories	Description		
	ASTM 2013	JGS 2003	BS 2009
Freezing type	One way	One way	One way
Freezing temperature	-12 ± 0.1 °C	-10 ± 0.1 °C	-17 ± 1 °C
Freezing direction	Top to bottom	Bottom to top	Top to bottom
Water supply condition	Open system (bottom)	Open system (top)	Open system (bottom)
Material of mold	Acryl	Acryl	Brass
Size of the sample	146 mm in diameter	60 mm in diameter	101.6 mm in diameter
	150 mm in height	20 to 40 mm in height	152.4 mm in height
Surcharge	3.5 kN/m ²	–	–

apparatus reach uncertainty of 3% or more for particles finer than 20 mm. Moreover, the apparatus can only simulate one-way freezing from the top (-12 ± 0.1 °C) to the bottom ($\geq 0 \pm 0.1$ °C), although it does have the options of being with or without a water supply at the base. The Japan Geotechnical Society (JGS 2003) recommended the use of undisturbed samples or soil composed of particles < 19 mm. As indicated in Fig. 1b, the JGS can simulate one-way freezing as the ASTM apparatus does, but the JGS adopts an opposite freezing direction: from the bottom (-10 ± 0.1 °C) to the top ($\geq 0 \pm 0.1$ °C). Additionally, it has an open system for the water supply. The British Standard [18] similarly suggests testing soils composed of particles finer than 19 mm. The device can simulate one-way freezing with the direction of freezing from the top (freezing air -17 ± 1 °C) to the bottom (4 ± 0.5 °C) and also has a water supply available at the base, as shown in Fig. 1c.

Although several testing apparatuses that can conduct frost-heave tests have been used, they still have some limitations. Test standards by the ASTM, JGS, and BS only simulate unidirectional freezing and two of them cannot observe movement of the soil structure during the test (the exception is the JGS). All these methods are very costly for the following reasons: a temperature controllable chamber is required, much effort is required for the experimental setup, and these methods still cannot measure the frost-heave expansion pressure [16–18]. Lay [19] developed a frost-heave testing device that consists of a single-bath container that assists simultaneous testing of nine samples but this apparatus was very similar to the ASTM, JGS, and BS standards in that it used a temperature controllable chamber in which it was not possible to observe changes in

the sample during the test. Furthermore, numerous laboratory testing devices [10, 20, 21] do not allow observation of physical changes due to the insulation around the cell. To overcome this situation, new frost-heave test equipment was invented by Dagil [22], but this testing device also utilized a cooling chamber to simulate a constant temperature in the surroundings. Recently, Jin et al. [23] presented a simple frost-heave testing device using a temperature-controlled cell. This device used a fixed cell (the cell and bottom plate were fixed). However, when the test was performed in the downward freezing direction, the frost-heave amount was moderately low compared to the estimation, and the connection between the cell and bottom plate broke, because it was influenced by the adfreezing bond between the frozen soil and the inner cell. Therefore, more studies on a frost-heave test apparatus should be considered regarding the development of temperature control and measurement of the frost-heaving expansion pressure.

In this study, a new apparatus for testing frost-heave with multiple functions was developed that resolves the issues of the existing frost-heave test devices. This new device can control the boundary temperatures with high accuracy, exert overburden pressure, and can also control the loading condition, with and without vertical deformation, to measure the amount of frost-heave and heaving pressure separately. The accuracy of the results obtained from the new device was validated by theoretical estimates.

2 Development of a Frost-Heave Testing Apparatus with a Triple Cell

2.1 Acrylic Cylindrical Triple Cell

Figure 2 shows a schematic diagram of a newly developed frost-heave testing device that considers various testing conditions. The apparatus consists of a frost-heave cell (triple cell), a thermal bath system, water supply system, a displacement measurement system, a load cell, a hydraulic cylinder, and a data acquisition system. The specifications of the newly developed testing apparatus with three nested acrylic cylinders are summarized in Table 2. The specimen dimensions, the height in particular, can impact the frost-heave rate. Moreover, due to the adfreeze force by the frozen soil on the inner wall, sample dimensions of 100 mm (height and diameter) were used in this study [15, 22, 23].

The cell was made of transparent acryl, which has low thermal conductivity and enables visual confirmation of sample deformation. Moreover, it is a moving cell (top plate, bottom plate, and triple cell not fixed to each other), which enables the cell to move freely in vertical directions.

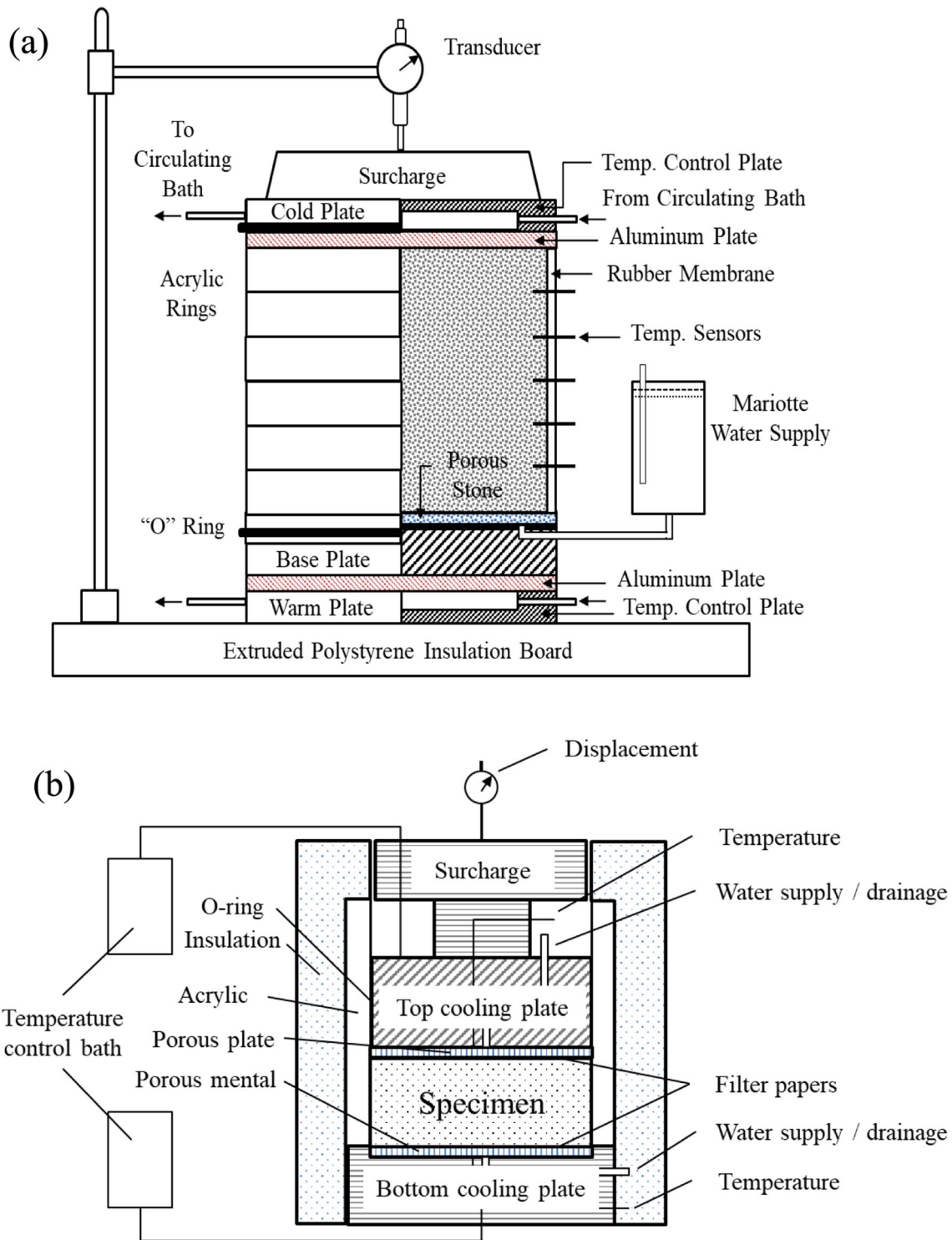


Fig. 1 Schematic of the three kinds of frost-heave apparatus: a ASTM, b JGS, c BS

The triple cell also enables accurate control of the boundary temperature and prevents heat transfer between the soil sample and the ambient air, as shown in Fig. 3. The triple cell consists of three separate cells (each one 10-mm thick) with 10-mm spaces between them. The outer cell is

connected to a vacuum pump to prevent heat extraction by convection and conduction. The gap between the inner and middle cell is connected to a thermal bath system to apply a constant temperature to the sample perimeter. The inner

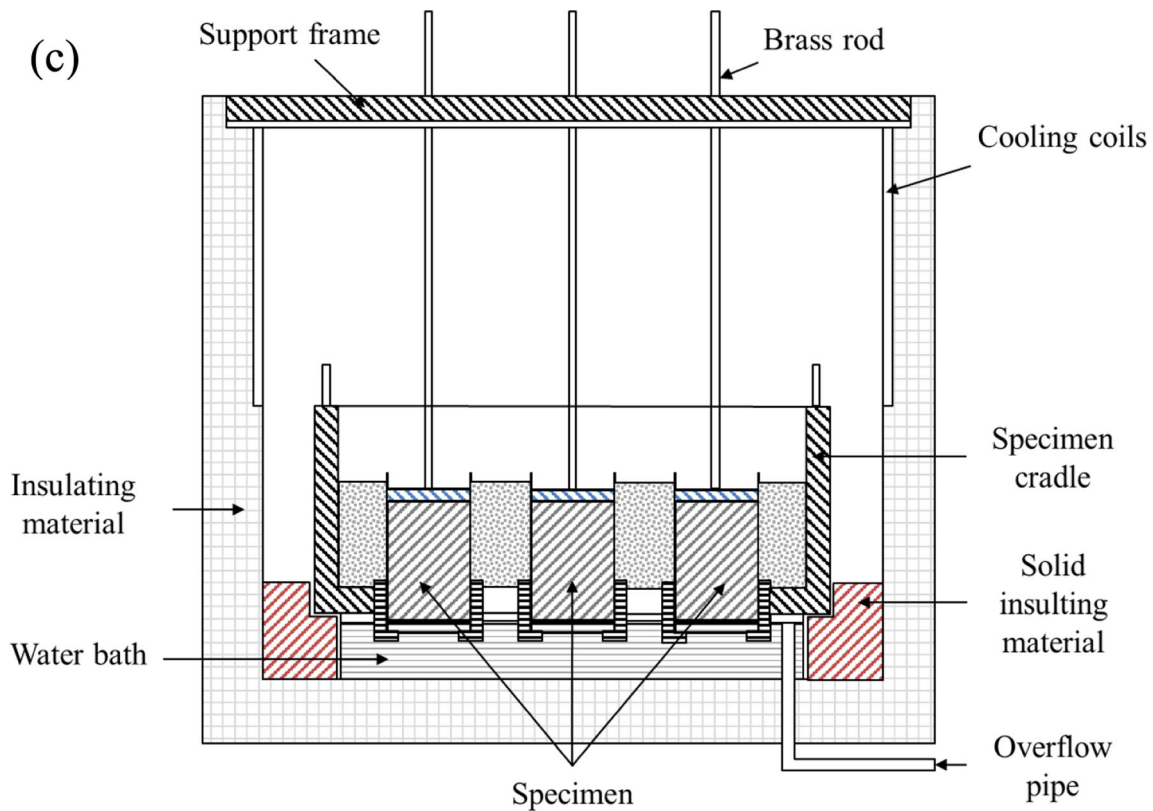


Fig. 1 continued

cell has dimensions of $100 \times 385 \times 10$ mm (diameter, height, and thickness).

The top plate and bottom plates were made of aluminum, as shown in Fig. 3. Both plates have three holes, and two of the holes are utilized for circulation of the anti-freezing liquid and the third hole is used in the drainage system (Fig. 3). In the case of the top plate, another hole was made for installation of a thermocouple sensor at the top and bottom of the sample. The soil sample is placed inside the cell between the top and bottom cap.

2.2 Temperature Monitoring and Control Instruments

The thermal bath system consists of three separated cooling and heating units connected to the top plate, the bottom plate, and the surrounding cell. In this study, a circulatory cooling and heating system was used to circulate the anti-freezing liquid (ethylene glycol-to-water ratio of 1:1) through the top plate, bottom plate, and acrylic cell. The thermal system has a controllable temperature range from -33 to 40 °C with a precision of ± 0.1 °C. The circulation tube has a diameter of 15 mm and is wrapped with insulation to minimize heat loss during freezing and thawing, as shown in Fig. 4a–d. To measure the temperature, eight T-type thermocouples were installed at the top

and bottom of the sample, at the inlet and outlet of the top plate, on the bottom plate, and in the cell as shown in Fig. 4. Additionally, a 50-mL burette was connected to the bottom plate enabling the inflow or outflow of water (~ 5 mL/min) as a water supply system [24]. A laser displacement sensor was added to measure change in the height of the sample during experiments with an accuracy of ~ 0.01 mm. A load cell with the maximum capacity of 5.9 kN with 1% accuracy was also used. The newly developed system can be set up for two types of load control modes: load control on (free moving bar for measuring the frost-heave deformation) and load control off (fixed loading bar for measuring the heaving pressure). The loading bar (maximum capacity of 78.5 kN) is used to apply an external load to simulate overburden pressure on the top of a specimen. All the sensors (load cell, laser displacement, hydraulic cylinder, and thermocouples) were connected to a data acquisition system that collected data automatically every minute.

2.3 Temperature Control

In the actual field, the ground temperature is greatly affected by the atmospheric (and ground surface) temperatures, the heat flow into the ground, and the thermal properties of the soil [2]. However, it is difficult to simulate

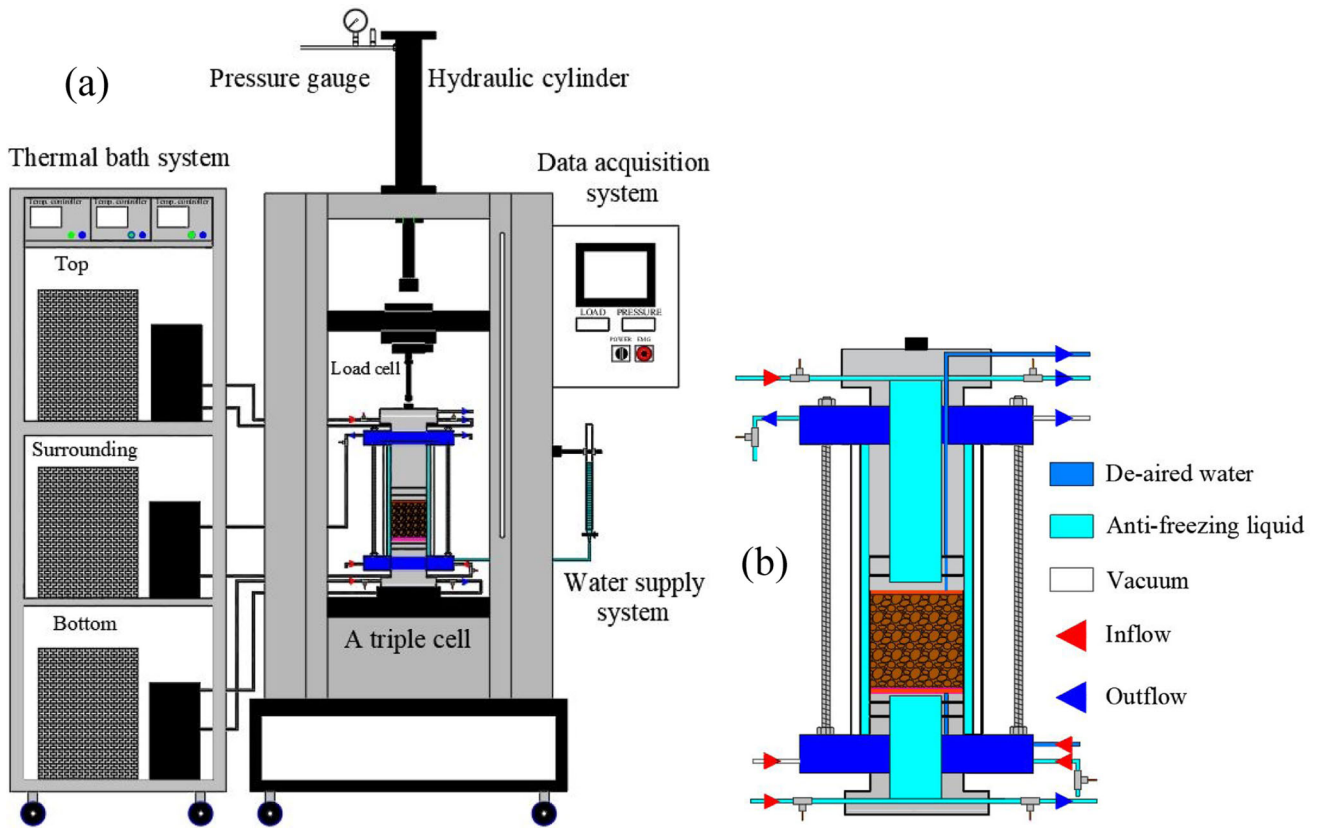


Fig. 2 Schematic diagram of the frost-heave test: **a** frost-heave testing machine and **b** triple cell

Table 2 Characteristics of the frost-heave test apparatus

Categories	Description
Cell type	Triple cell
Minimum control temperature	$-15 \pm 0.1 \text{ }^\circ\text{C}$
Direction of freezing	Top to bottom
	Both side (top and bottom)
	Bottom to top
Water supply condition	Open and closed system
Load control mode	On (displacement unfixed)
	Off (displacement fixed)
Material of mold	Transparent acrylic
Size of the sample	100 mm in diameter and height
Overburden pressure	10,000 kN/m ²

in the laboratory the same temperature distribution and thermal conditions that occur in the field. Therefore, in numerous studies by Zhang et al. [3], Wang et al. [10], and Jin et al. [23], frost-heave tests were performed using constant negative temperatures. To achieve the target temperature in the soil sample, the temperature calibration needed between the setting temperature of the device and the real temperature at the soil sample was evaluated. The

main reason for the temperature calibration is because the setting temperature from the thermal bath changes during its flow through the lines connected to the top and bottom plate and also to the surrounding acrylic cylinder for the boundary temperature. Generally, in laboratory tests, the temperature is controlled using the internal control mode, which is used to control the temperature of the inflowing liquid [9, 23]. With the same internal control mode, an additional step was applied for calibration of the soil temperature with high accuracy. To determine the upper soil temperature (T_u), a total of seven calibration tests were conducted. The temperature on the top plate of the device (T_m) was set at different values ($-5, -7.5, -10, -12.5, -15, -17.5$, and $-20 \text{ }^\circ\text{C}$). During the test, the room temperature was $\sim 20 \pm 2 \text{ }^\circ\text{C}$. Due to heat transfer from the top plate and the connecting lines, the applied T_m was not the same as T_u . Figure 5 shows the relationship between the setting temperature and the temperature of the top surface of the specimen. The result shows that T_u increases linearly as T_m increases. Based on this relationship, the temperature at the top surface of the sample can be exactly controlled using the setup temperature.

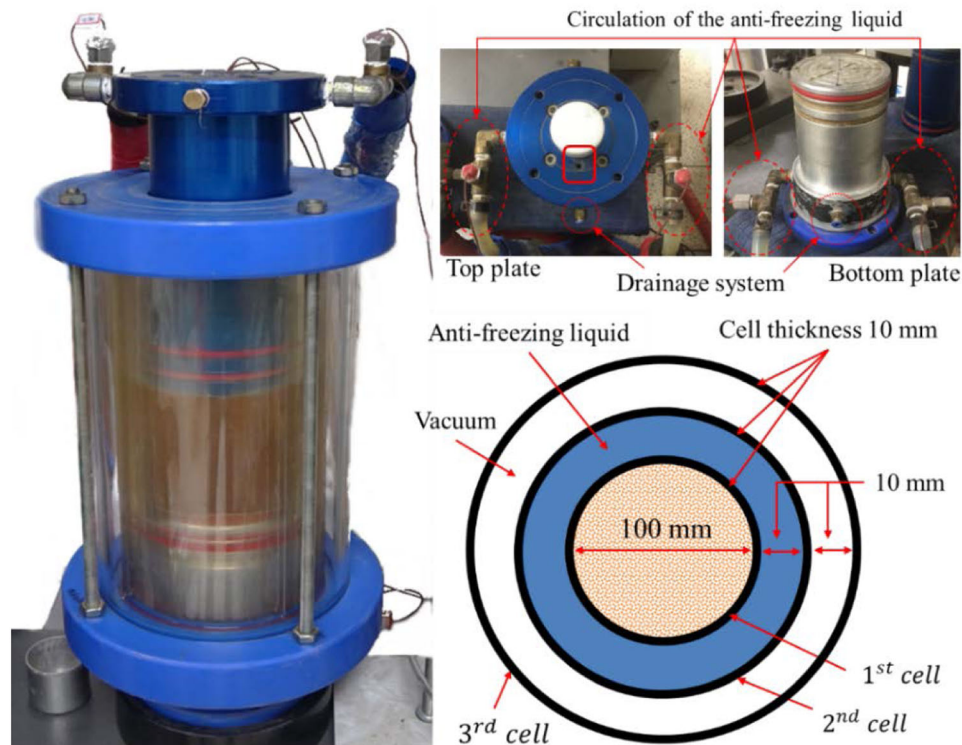


Fig. 3 The triple cell of the acrylic cylinder

3 Validation and Apparatus Control

3.1 Materials

To validate the performance of the new apparatus, a series of frost-heave tests were carried out using water-saturated Jumunjin standard sand (JSS). Although JSS is not a frost susceptible soil, it was selected, because the pore water would increase in volume by about 9% while freezing without a supply of additional water. Moreover, in previous research, JSS was selected for the validation of an older frost-heave testing device as well [23]. The grain size distribution of the soil sample used in the study is shown in Fig. 6. The specific gravity of the sand (G_s) was 2.67 [25]. The maximum ($\gamma_{d,max}$) and minimum ($\gamma_{d,min}$) dry unit weight of JSS is 16.5 and 13.3 kN/m³, respectively, in accordance with ASTM D 4253-14 [26] and ASTM D 4253-14 [27]. According to the Unified Soil Classification System (USCS) [28], JSS is classified as a poorly graded sand (SP).

3.2 Sample Preparation and Test Methods

We performed a series of one-directional freezing experiments to validate the frost-heave testing device. The sample preparation and test methods adopted herein were based on the ASTM [16] and Jin et al. [23]. The step-freezing

boundary condition was also used in this study [29]. A reconstituted cylindrical soil sample 100 mm in height and 100 mm in diameter was prepared with 90% compaction in relative density based on its $\gamma_{d,max}$ and $\gamma_{d,min}$. A predetermined amount of dry sand was compacted in three layers, with a small metal tamper weighting 300 g to achieve a homogenous condition. To minimize the wall friction between the top plate, bottom plate, and the inner sidewall of the acrylic cell, and between the inner acrylic cell and the frozen soil, silicone grease (Shin-Etsu G-40M) was applied. The frost-heave tests of fully saturated JSS were performed in a closed system (without water supply and without drainage at the top and bottom) following three main steps. After preparation of a specimen, the 50-mL burette was connected to the bottom plate, which enabled water inflow (about 5 mL/min) to the specimen. The flow was maintained for 6 h to ensure full saturation of the specimen. To remove air in the soil sample, a vacuum (-98.7 kN/m²) was applied for approximately an hour. After the soil sample was fully saturated, the valve for the inflow of water was closed to provide the undrained condition. A surcharge of 1.27 kN/m² was applied to the top plate as a seating pressure; then, an initial temperature of 3 °C was applied as a boundary condition for 24 h. Next, the freezing temperature was applied for 24 h to investigate the frost-heave properties of JSS.

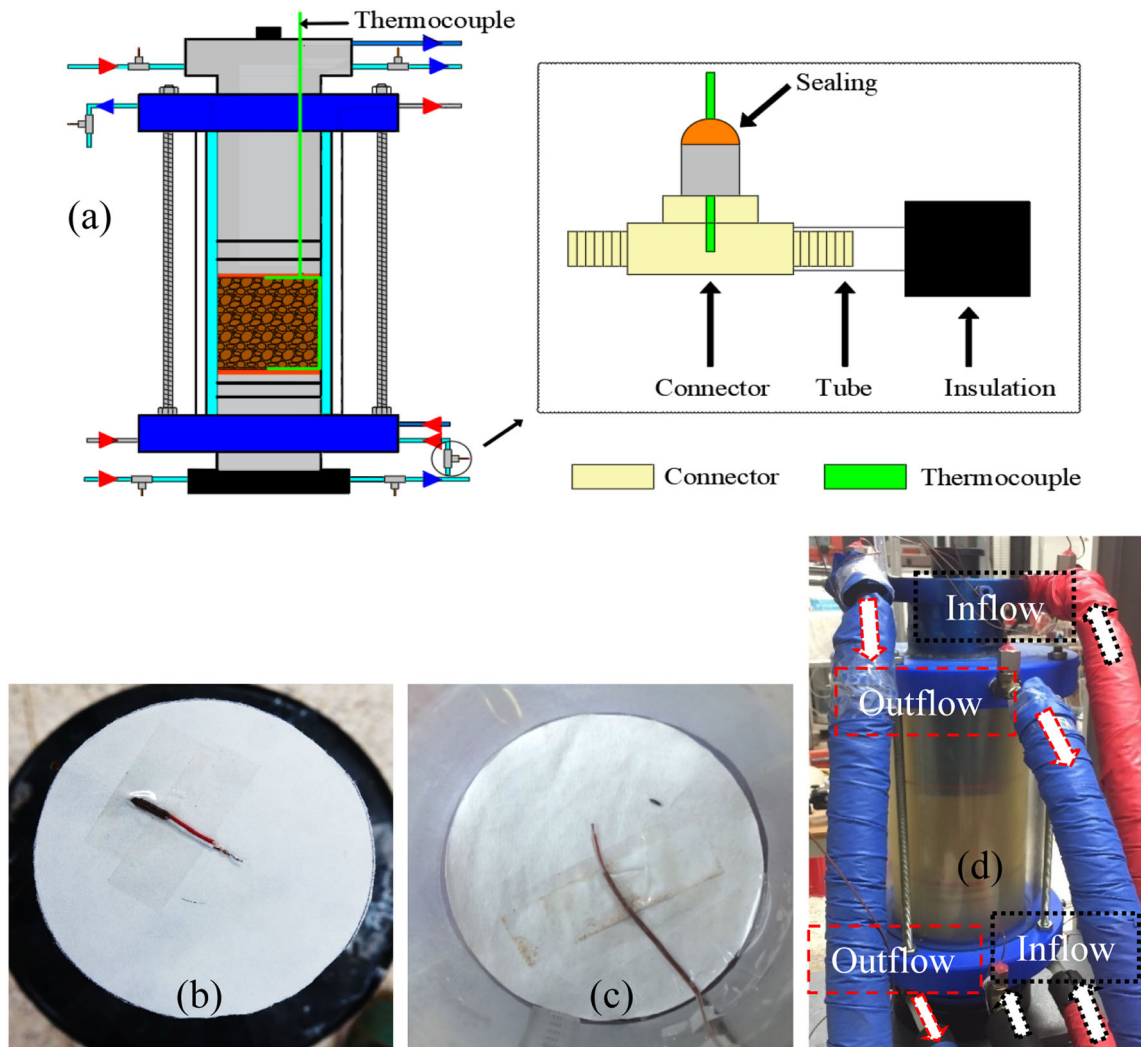


Fig. 4 Installation of the thermocouples and insulation: a schematic diagram, b top plate, c bottom plate, and d insulated lines

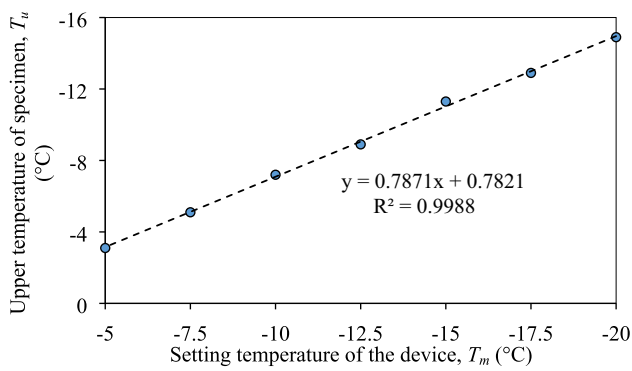


Fig. 5 Temperature control of the frost-heave test apparatus

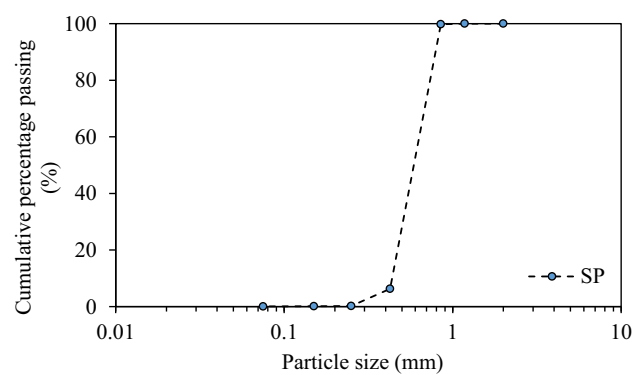


Fig. 6 Grain size distribution of the JSS

3.3 Estimation of Frost-Heave Amount

As mentioned above, during the freezing process, the pore water turns into pore ice with 9% volume expansion. To estimate the amount of frost-heave amount in this study,

three parameters (volume of water intake required for complete saturation of the specimen, frost length, and porosity of the sample) were used in the following equation:

$$\Delta h = 0.09 \cdot n \cdot H_f, \quad (1)$$

where Δh is the frost-heave amount; n is the porosity of soil sample; and H_f is the frost length.

During the frost-heave test, the frost-heave ratio was evaluated. The frost-heave ratio is a function of the frost-heave amount and the frost length in a certain period determined by the following Eq. (2) [10]:

$$\eta = \frac{\Delta h}{H_f} \times 100\%, \quad (2)$$

where η is the frost-heave ratio; Δh is the frost-heave amount; and H_f is the frost length of the specimen.

4 Analysis of the Frost-Heave Amount and Heaving Pressure

4.1 Effect of a Single and Multiple Cells

During the process of soil freezing in the vertical direction, side insulation is an important factor in forming an ice lens. To solve this problem, previous studies circulated an anti-freezing liquid of a certain temperature around the specimen, but its effectiveness was not well-documented. In this study, a vacuum was applied between the third and second cell, and an anti-freezing liquid was circulated between the second and first cell to maintain a constant surrounding temperature. To study the effect of multiple cylindrical cells on the frost-heave properties, a series of the frost-heave tests using saturated JSS was conducted using a triple cell, double cell (the third cell was removed), and single cell (the third and second cells were removed) device, as shown in Fig. 7 and Table 3. The sample preparation and test procedures were the same as mentioned above, using the freezing direction from top to bottom and a freezing temperature of $-10\text{ }^\circ\text{C}$.

4.1.1 Soil Temperature Change

To investigate the effect of the single cell and multiple cells (double or triple cell) on the temperature at the top, bottom, and surrounding area of the specimen, thermocouples were installed at the center of the top and bottom

Table 3 Test conditions of the frost-heave test

Test condition	Freezing direction	Initial temp. ($^\circ\text{C}$)	Controlled temp. ($^\circ\text{C}$)		
			Top	Bottom	Surrounding
Triple	Top to bottom	3	–	3	3
Double			10	3	
Single			–	–	

of the sample and at the inflow and outflow circulation lines for the anti-freezing liquid. Based on the results of the temperature control shown in Fig. 5, a T_m of about $-13.7\text{ }^\circ\text{C}$ was applied to achieve a T_u of $-10\text{ }^\circ\text{C}$. Figure 8 presents the temperature measured at the upper, lower, and surrounding area of the soil specimen in the triple cell, double cell, and single cell. The temperature change behavior at the top of the specimen could be divided into three stages [30]: a fast cooling stage (FCS), slow cooling stage (SCS), and stable stage (SS). In the initial state, it can clearly be seen that the upper soil temperature dramatically decreases at the early stage and reaches the stable stage after 300 min. By applying a negative temperature at the top, the heat transfer in the soil sample was influenced, and the soil temperature on the opposite side decreased. Thus, the lower soil temperature (T_l) slightly decreased from $3\text{ }^\circ\text{C}$ (initial temperature boundary condition) to about $1.7\text{ }^\circ\text{C}$ under the effect of the constant temperature of the bottom plate, within 1440 min.

From Fig. 8b, it was noted that the surrounding temperature of the soil sample shows a little fluctuation ($\sim 3 \pm 0.4\text{ }^\circ\text{C}$) because of the use of a double cell (with the outer cell removed). The upper and lower soil temperature in all three conditions showed almost the same trend during the testing period, even for the single cell. The similarity of the trends was due to the thermocouples being in direct contact with the top and bottom cooling plate (Fig. 4); however, the single cell (with outer and middle cells removed) had the highest heat loss during the experiment (Fig. 8c). To calculate the frost length of the soil sample, a linear distribution of the temperature was assumed based on the measured soil temperature after freezing it for 24 h [16–19]. Therefore, the soil sample

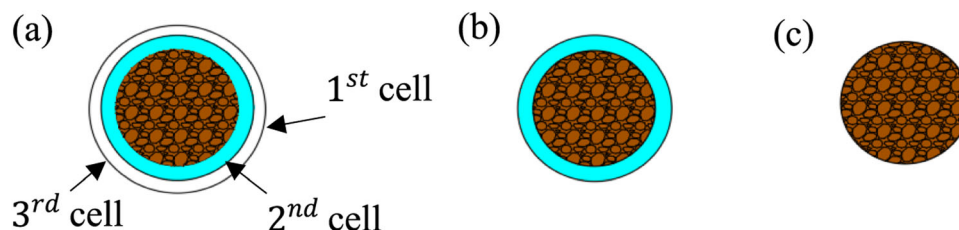


Fig. 7 Test condition of the frost-heave test: **a** triple cell, **b** double cell, and **c** single cell

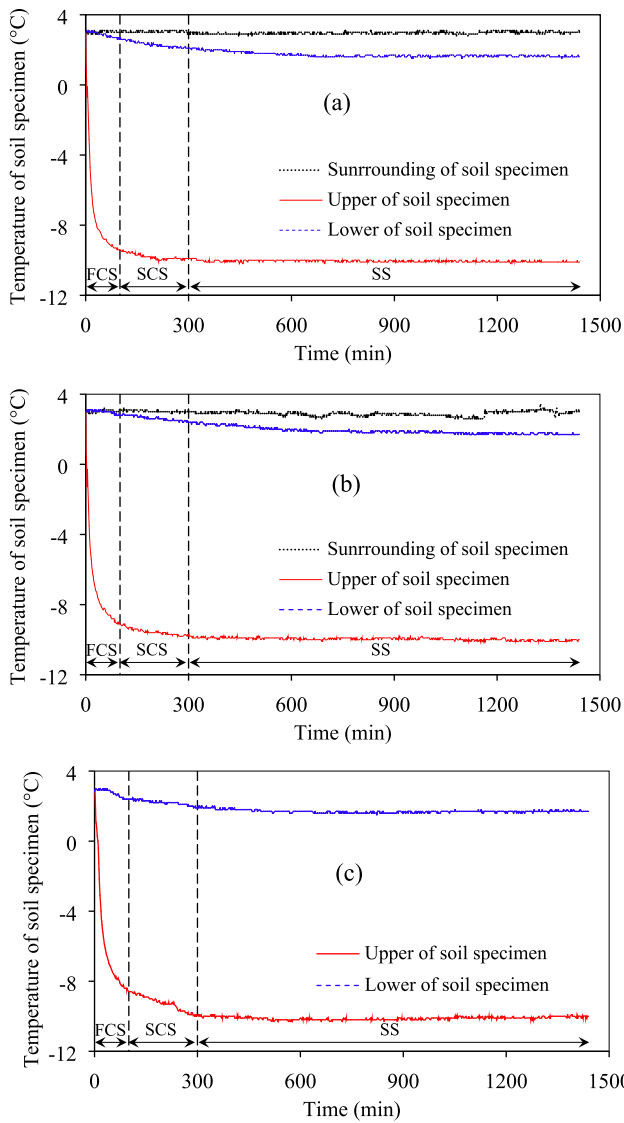


Fig. 8 Soil temperature results by time interval: **a** triple cell, **b** double cell, and **c** single cell

could be separated into a frozen and unfrozen part based on the spatial distribution of the temperature. Moreover, the temperature gradient (the temperature difference between the top and bottom of the specimen over the height of the specimen) was determined and the results were 0.113, 0.114, 0.114 °C/m, whereas the proposed ASTM, JGS, and BS gradient temperature was about 0.04, 0.25, and 0.14 °C/m, respectively [16–18]. The frost length and frost-heave ratio, determined for each case based on the soil temperature measurement, are listed in Table 4.

4.1.2 Frost-Heave Amount

The initial water content of the specimen is an important determinant of the amount of frost-heave in a closed

Table 4 Frost-heave test results for soil-type JSS

Test condition	Vol. of water (mL)	H_f (mm)	η (%)	Δh (mm)		Error (%)
				Estimated	Measured	
Triple cell	308.27	85.47	3.37	3.019	2.881	4.58
Double cell	312.82	85.47	3.39	3.064	2.901	5.31
Single cell	313.00	85.47	2.75	3.066	2.306	24.78

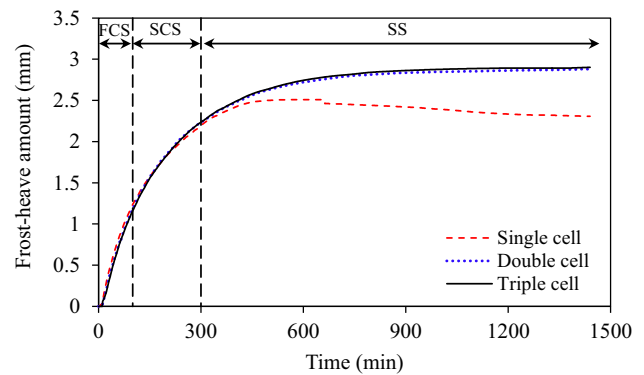
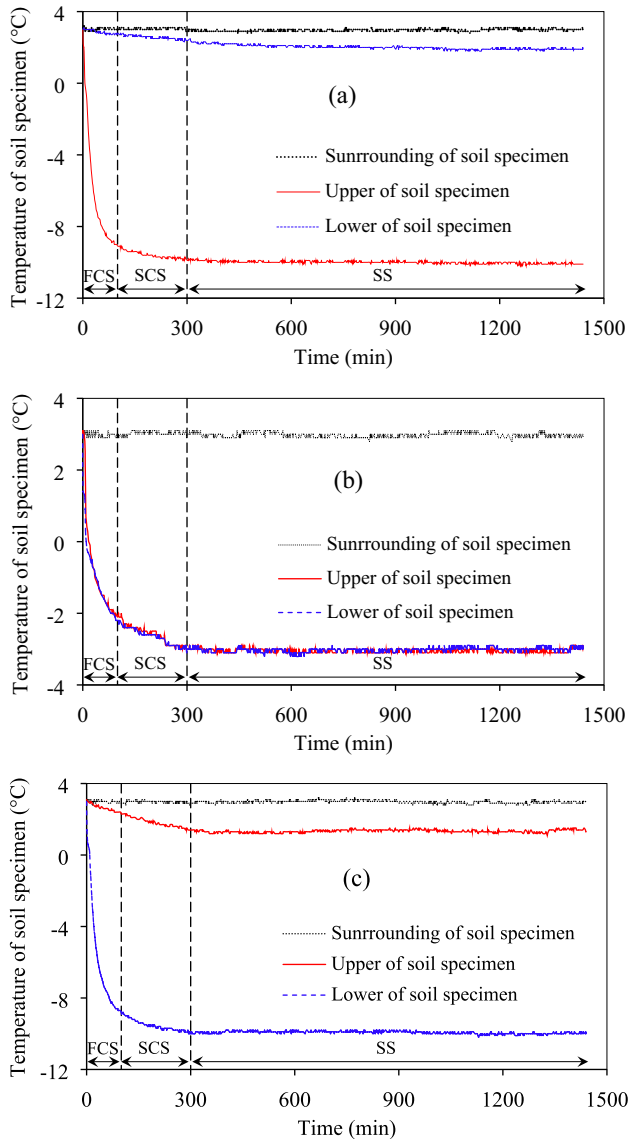


Fig. 9 Frost-heave amount in the newly developed devices

system. Almost identical initial conditions were achieved in each test, with < 0.4% difference in the water content of the saturated soil in the triple, double, and single cell (24.47, 24.83, and 24.84%). This corresponded to 308.27, 312.82, and 313.00 mL, respectively. Figure 9 shows the result for the frost-heave amount (Δh) using the triple, double, and single cell. The error between the estimated and measured frost-heave is summarized in Table 4. The amount of frost-heave was estimated using Eq. (1), based on the volume of water in the soil sample, of which the volume expands by 9% as the pore water changes to pore ice. With the same initial height and temperature boundaries, the frost length of the three specimens was the same while the frost-heave ratio η was different according to the water content. In Fig. 9, it can clearly be seen that the Δh for the triple and double cells rapidly increased until 600 min, and then were constant, with only a slight increase until the end of the test. Due to higher fluctuation of the surrounding temperature in the double cell (± 0.4 °C) compared to the triple cell (± 0.1 °C), the error value between the measured and estimated frost-heave for the double cell is higher than that of the triple cell in Table 4. Thus, it can be concluded that the triple cell provides better side insulation and accordingly, better temperature control, than the double cell does.

Table 5 Experimental conditions of the frost-heave tests

Freezing direction	Initial temperature (°C)	Controlled temp. (°C)		Sample condition	Water supply
		Top	Bottom		
Top to bottom	3	− 10	3	Saturated	Closed system
Both sides		− 3			
Bottom to top		3	− 10		

**Fig. 10** Measured temperature over time for different freezing directions: **a** top to bottom, **b** both sides, and **c** bottom to top

Interestingly, apart from the results of the double and triple cells, the curve representing the Δh for a single cell, shows a slight decrease after the peak frost-heave and until the end of the test. The error value is also the largest (by about 5.41 and 4.66 times) compared to the error of the

triple and double cells, respectively. The error might be caused by heat transfer between the ambient air and the soil specimen through the single acrylic cell and due to incomplete saturation. Also different from a triple or double cell, both of which were kept under constant temperature by circulation of the anti-freezing liquid, the single acrylic cell could have temperature variation and accordingly, a slight change in diameter, which could have resulted in the higher error noted in its frost-heave. Based on this result, to prevent an effect from ambient temperature on the frost-heave, a frost-heave testing apparatus with a triple cell, or at least a double cell, is recommended for such experiments.

4.2 Effect of the Freezing Direction

The freezing direction, in nature, is generally from the surface to the bottom of the soil. The nature of the frost phenomenon can be simulated in the experiment by setting the freezing direction from top to bottom. However, the adfreeze forces between the specimen and the inside cell wall can hinder the vertical movement of the freezing specimen. Therefore, the bottom to top freezing direction was used to enable soil expansion at the top [17, 19], even though this direction is the opposite of the natural condition. To solve this problem, the apparatus in this study was designed to freeze the sample from the top to the bottom, the bottom to the top, and in both directions simultaneously, using three moving cells. Three tests for fully saturated JSS were conducted to investigate the effect of the freezing direction on the frost-heave properties, as shown in Table 5. The sample preparation and test methods were the same as mentioned before, and the triple cell was used for the experiment.

4.2.1 Soil Temperature Change

Figure 10 shows the relationship between the change in soil temperature (top, bottom, and surrounding) with time. As shown in this figure, the soil temperature rapidly decreases and reaches a stable temperature after 300 min of being subjected to a freezing temperature. For a freezing temperature of -3°C , in the case of freezing from both sides, the soil sample was fully frozen. The frost length and the frost-heave ratio (in each case) were determined based on the resulting change of the soil temperature, as summarized in Table 5.

4.2.2 Frost-Heave Amount

Figure 11 shows the relationship between the frost-heave amount and the elapsed time of the JSS. The test results show that Δh gradually increases and becomes constant

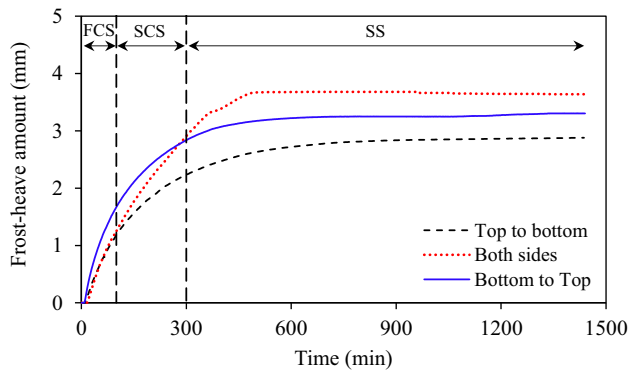


Fig. 11 Frost-heave amount of the JSS

Table 6 Frost-heave test results of the JSS

Freezing direction	Vol. of water (mL)	H_f (mm)	η (%)	Δh (mm)		Error (%)
				Estimated	Measured	
Top to bottom	308.27	85.47	3.37	3.019	2.881	4.58
Both sides	313.27	100.00	3.64	3.590	3.638	1.34
Bottom to top	314.14	87.72	3.77	3.158	3.303	4.60

after about 500 min. From this, it can clearly be seen that, during the freezing process, Δh is a function of the negative temperature and the amount of water in the soil sample. In contrast, the effect of wall friction is insignificant, because silicone grease was applied between the inner acrylic cell and the frozen soil. Based on the volume expansion of the pore water to pore ice, which was $\sim 9\%$, the frost-heave amount in the soil sample was estimated. The comparison between the estimated and measured Δh using saturated JSS is summarized in Table 6. From this table, it can be seen that the measured value of Δh for freezing from top to bottom was lower than estimated; but in the case of the

Table 7 Frost-heave test conditions for temperature control

Designation	Freezing direction	Initial temp. (°C)	Controlled temp. (°C)		Temp. gradient (°C/mm)	Sample condition	Water supply	Load control mode
			Top	Bottom				
TB_0.09	Top to bottom	3	-6	3	0.09	Saturated	Closed system	Free and fixed
°C/mm								
TB_0.11			-8	0.11				
°C/mm								
TB_0.13	-10	0.13						
°C/mm								

freezing direction from bottom to top, the measured value was higher than the estimated value. This could be an effect from the initial saturation level and gravity on the water in the soil, while the added weight of the cell caused by the adfreeze force was negligible. This was because the pressure caused by the cell weight was less than 1 kN/m^2 . The experimental results show that the error of these three cases was $< 6.27\%$. The newly developed frost-heave apparatus showed good performance compared to that in a previous study by Jin et al. [23] where the connection between the cell and bottom plate broke during the testing in the downward freezing direction. This problem was due to the adfreezing effect creating a force on the fixed bottom plate.

4.3 Effect of the Temperature Gradient

Six frost-heave tests using the triple cell were performed with freezing direction top to bottom for various temperature gradients (i.e., 0.09, 0.11, and 0.13 °C/mm) as shown in Table 7. Two additional types of load control modes (Table 2) were used for the newly developed triple cell frost-heave testing device, which could measure both the frost-heave amount (free) or the heaving pressure (fixed). The test was conducted with a closed system and a specimen of fully saturated JSS by applying a freezing temperature for 24 h. Then, the error between the measured and estimated results was examined.

4.3.1 Soil Temperature Change

To apply an accurate temperature of -6 , -8 , and -10 °C at the top of the specimen, the setting temperature of the device was controlled based on the results in Fig. 5. Figure 12 shows the change in temperature at the top of the specimen, and the error of the top temperature of the specimen was only about 0.00, 0.00, and 0.99% for -6 , -8 , and -10 °C, respectively. In Fig. 12, the upper soil temperature gradually decreased from the initial

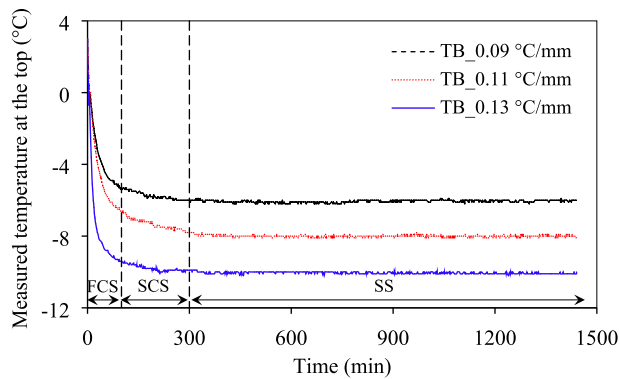


Fig. 12 Temperature change at the top of the specimen

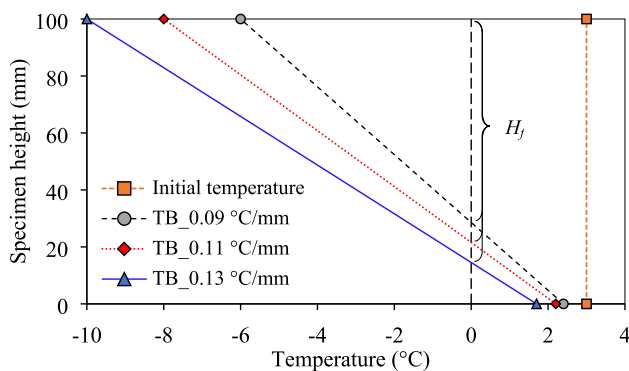


Fig. 13 Linear soil temperature profile after 24 h based on the measured top and bottom of the specimen

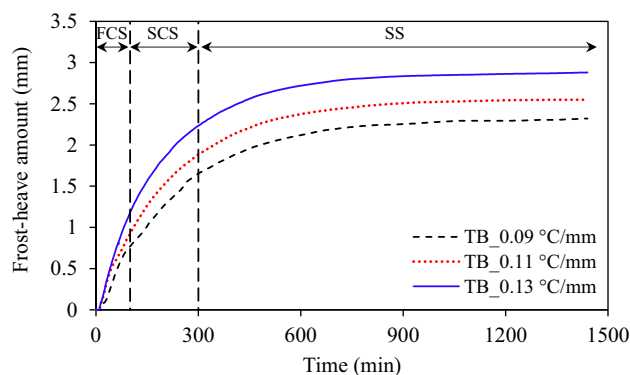


Fig. 14 Results of the frost-heave amount

temperature (3 °C) and reached a stable stage within 300 min. As the controlled temperature at the top decreased from -6 to -10 °C, the interval needed to reach a maximum and stable temperature was almost the same; moreover, the frost length increased with decreasing temperature. The testing was carried out with an initial temperature of 3 °C in the whole specimen. However, due to the influence of the negative temperature at the top of the specimen, the bottom temperature decreased to between 1.7 and 2.4 °C. As mentioned above, to estimate the frost

length, the linear distribution of the temperature from top to bottom of the sample was assumed, as indicated in Fig. 13. From this, the temperature gradient of the present test results (after 24 h) decreased about 0.002, 0.0027, and 0.0036 °C/mm for the freezing temperature 0.09, 0.11, and 0.13 °C/mm, respectively, which is within the range of the international standard [16–18]. The results of the frost length and the frost-heave ratio are summarized in Table 7.

4.3.2 Frost-Heave Amount

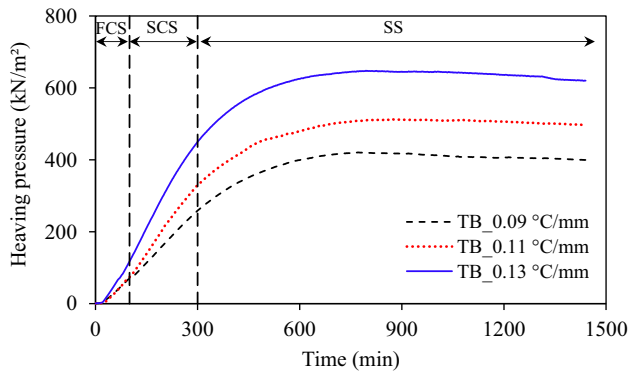
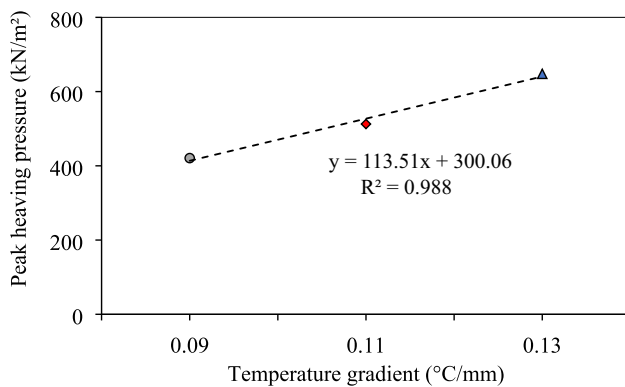
To investigate the effect of the freezing temperature on the frost-heave amount of JSS, three tests were performed using the function of the load control in the “on mode” (Table 2, unfixed displacement). Figure 14 and Table 8 show the change in the amount of frost-heave over time for different freezing temperatures. It can be seen that the heaving amount of the JSS increased with increase in the temperature gradient from 0.09 to 0.13 °C/mm. In the early state, the heaving amount of JSS rapidly increased and then rose only slightly after 600 min. Compared with the temperature change shown in Fig. 12, where the upper soil temperature reaches a stable state within 300 min, the frost-heave of the JSS still shows a very high increase in rate even at 300 min. After 600 min, the frost-heave rate slightly decreases because the test was conducted in a closed system, which led to an insufficient water supply. A comparison between the measured and estimated results is presented in Table 8, and the error of the measured frost-heave decreases (from 7.40 to 4.58%) with decrease in the temperature. Based on these results, the testing device is expected to give a fairly accurate frost-heave estimation even for the downward freezing direction when subjected to the standard freezing temperature in the ASTM (-12 °C), JGS (-10 °C), and BS (-17 °C) devices.

4.3.3 Frost-Heave Expansion Pressure

A series of tests were conducted to determine the frost-heaving expansion pressure using the function of the load control in the “off mode” (Table 2, fixed displacement). Figure 15 shows the result of the heaving pressure of JSS over time in different temperature gradients. By applying the different temperature gradients (different freezing temperature on the top of a soil sample), the pressure gradually increased to the peak value and then slightly decreased after ~ 800 min. This increasing pressure was due to the expansion of the ice caused by the freezing temperature. After reaching the peak pressure, the heaving pressure leveled off through the end of the test, which might be caused by stress relaxation, while the temperature in the specimen became stable and reached a constant value. These experimental results were consistent with

Table 8 Frost-heave test results of the JSS

Designation	Freezing direction	Vol. of water (ml)	H_f (mm)	η (%)	Δh (mm)		Error (%)
					Estimated	Measured	
TB_0.09 °C/mm	Top to bottom	306.21	71.43	3.25	2.506	2.321	7.40
TB_0.11 °C/mm		310.62	78.43	3.25	2.792	2.549	8.69
TB_0.13 °C/mm		308.27	85.47	3.37	3.019	2.881	4.58

**Fig. 15** Heaving pressure over time**Fig. 16** Maximum heaving pressure

those in a previous study [31]. If the maximum heaving pressure is plotted with the freezing temperature (Fig. 16), it can be seen that the maximum heaving pressure increases inversely with the freezing temperature. The difference in the maximum heaving pressure of saturated JSS for the temperature gradients of 0.09 and 0.11 °C/mm and 0.09 and 0.13 °C/mm was about 1.22 and 1.60 times, respectively.

5 Conclusions

In this paper, a new frost-heave testing device was developed. The testing device can achieve high accuracy for temperature control and for testing in various freezing

directions using multiple, movable cells. Both the frost-heave amount and the heaving pressure can be measured due to inclusion of two types of load control function (free and fixed loading bar). We performed a series of experiments by considering multiple cells (triple cell, double cell, and single cell) and freezing direction (top to bottom, both ends to center, and bottom to top). Furthermore, the effect of various freezing temperatures was also considered for the freezing direction top to bottom. As the temperature gradient decreased from 0.09 to 0.13 °C, the frost-heave amount slightly increased to 2.881 mm for the free-loading bar, while the heaving pressure increased up to 647.82 kN/m² for the fixed loading bar. The newly developed testing device showed accurate estimation of the frost-heave amount compared to the theoretical result under various freezing conditions, with an error < 8.5%. Therefore, it can be concluded that this newly developed frost-heave testing device is suitable for use as a multi-purpose device under various test conditions to investigate the frost-heave properties of soils. Further research will be needed to investigate the frost-heave characteristics of frost susceptible soils in Gangwon Province, the coldest region in South Korea, using the newly developed frost-heave testing apparatus.

Acknowledgements This research was supported by a Grant (19RDRP-B103397) from the Regional Development Research program, funded by the Ministry of Land, Infrastructure and Transport of the Korea government.

References

- Penner E (1962) Ground freezing and frost heaving. National Research Council of Canada, Canadian Building Digest; no. CBD-26, pp 1–5. <https://doi.org/10.4224/40000788>
- Andersland OB, Ladanyi B (2013) An introduction to frozen ground engineering. Chapman & Hall, New York
- Zhang M, Zhang X, Li S, Lu J, Pei W (2017) Effect of temperature gradients on the frost heave of a saturated silty clay with a water supply. *J Cold Reg Eng* 31(4):1–11. [https://doi.org/10.1061/\(ASCE\)CR.1943-5495.0000137](https://doi.org/10.1061/(ASCE)CR.1943-5495.0000137)
- Brandl H (2008) Freezing-thawing behavior of soils and unbound road layers. *Slo J Civ Eng* 16(3):4–12
- Kim DL, Lee YN (2005) Countermeasures for frost protection of tunnel lining. In: Proceedings of Korean Society of Civil Engineers Conference, Jeju, South Korea. 20–21 October 2005 (**In Korea**)

6. MOLIT (Ministry of Land, Infrastructure and Transport of Korea) (2013) Development of design and construction guidelines and management techniques for geotechnical structures to reduce the freeze damage in the region. Sejong, South Korea (**In Korea**)
7. Inokuma AI, Inano S (1996) Road tunnels in Japan: deterioration and countermeasures. *Tunn Underg Space Technol* 11(3):305–309. [https://doi.org/10.1016/0886-7798\(96\)00026-0](https://doi.org/10.1016/0886-7798(96)00026-0)
8. Konrad JM, Lemieux N (2005) Influence of fines on frost heave characteristics of a well-graded base-course material. *Can Geotech J* 42(2):515–527. <https://doi.org/10.1139/t04-115>
9. Konrad JM (2008) Freezing-induced water migration in compacted base-course materials. *Can Geotech J* 45(7):895–909. <https://doi.org/10.1139/T08-024>
10. Wang T-L, Yue Z, Ma C, Wu Z (2014) An experimental study on the frost heave properties of coarse-grained soils. *Tran Geotech* 1(3):137–144. <https://doi.org/10.1016/j.trgeo.2014.06.007>
11. Akagawa S, Hori M, Sugawara J (2017) Frost heaving in ballast railway tracks. *Proc Eng* 189:547–553. <https://doi.org/10.1016/j.proeng.2017.05.087>
12. Oswell JM (2011) Pipelines in permafrost: geotechnical issues and lessons. *Can Geotech J* 48(1):1412–1431. <https://doi.org/10.1139/t11-045>
13. Zheng H, Kanie S, Niu F, Akagawa S, Li A (2016) Application of practical one-dimensional frost heave estimation method in two-dimensional situation. *Soils Found* 56(5):904–914. <https://doi.org/10.1016/j.sandf.2016.08.014>
14. Dashjamts D (2010) Research on geotechnical properties of frost heaving soil hazards on foundations in Ulaanbaatar area of Mongolia. In: *Proceedings of Inter For Strat Tech*. Ulsan, South Korea, pp 13–1. <https://doi.org/10.1109/IFOST.2010.5668061>
15. Zeinali A, Dagli D, Edeskär T (2016) Freezing-Thawing Laboratory Testing of Frost Susceptible Soils, In: *Proceedings of 17th Nordic Geotechnical Meeting*, Reykjavik, Iceland, pp 25–28
16. ASTM D 5918-13 (2013) Standard test method for frost heave and thaw weakening susceptibility of soil. ASTM International, West Conshohocken, pp 1–13
17. JGS 0171 (2003) Test method for frost heave prediction of soils. Japanese Society of Geotechnical Engineering Standard, Tokyo, pp 1–6
18. BS 812-124 (2009) Testing aggregates, part 124: method for determination of frost heave. BSI Standards Publication, London, pp 1–32
19. Lay RD (2005) Development of a frost heave test apparatus. Dissertation, Brigham Young University
20. Wang TL, Liu YJ, Yan H, Xu L (2015) An experimental study on the mechanical properties of silty soils under repeated freeze–thaw cycles. *Cold Reg Sci Technol* 112:51–65. <https://doi.org/10.1016/j.coldregions.2015.01.004>
21. Zhang L, Ma W, Yang C, Yuan C (2014) Investigation of the pore water pressures of coarse-grained sandy soil during open-system step-freezing and thawing tests. *Eng Geol* 181:233–248. <https://doi.org/10.1016/j.enggeo.2014.07.020>
22. Dagli D (2017) Laboratory investigations of frost action mechanisms in soils. Dissertation, Luleå University of Technology
23. Jin HW, Lee J, Ryu BH, Akagawa S (2019) Simple frost heave testing method using temperature-controlled cell. *Cold Reg Technol* 157:119–132. <https://doi.org/10.1016/j.coldregions.2018.09.011>
24. Zheng H, Kanie S, Li A (2016) Study on the relationship between fine content and frost heave in fine-coarse particles mixture. In: *Proceedings of 11th International Symposium on Cold Region Development (11th ISCORD)*, Incheon, South Korea, pp 18–20
25. ASTM D 854-14 (2014) Standard test method for specific gravity of soil solids by water pycnometer. ASTM International, West Conshohocken, pp 1–8
26. ASTM D 4253-14 (2014) Standard test methods for maximum index density and unit weight of soils using a vibratory table. ASTM International, West Conshohocken, pp 1–14
27. ASTM D 4254-14 (2014) Standard test method for minimum index density and unit weight of soils and calculation of relative density. ASTM International, West Conshohocken, pp 1–9
28. ASTM D 2487-11 (2011) Classification of soils for engineering purposes (Unified soil classification system). ASTM International, West Conshohocken, pp 1–12
29. Konrad J-M, Seto JTC (1994) Frost heave characteristics of undisturbed sensitive Champlain Sea clay. *Can Geotech J* 312:285–298. <https://doi.org/10.1139/t94-033>
30. Ji Y, Zhou G, Hall MR (2019) Frost heave and frost heaving-induced pressure under various restraints and thermal gradients during the coupled thermal-hydro processes in freezing soil. *Bul Eng Geol Environ* 78(5):3671–3683. <https://doi.org/10.1007/s10064-018-1345-z>
31. Smith MW, Onysko D (1990) Observations and significance of internal pressures in freezing soil. In: *Proceedings of 5th Canadian Permafrost Conference*. National Research Council Canada-Centre d'études nordiques, Université Laval, Quebec, Canada, pp 5–8